

Biophotonics sensor acclimatization to stem cells environment

Mukhzeer Mohamad Shahimin^{1,*}

¹Department of Electrical and Electronic Engineering, Faculty of Engineering, National Defence University of Malaysia (UPNM), Kem Sungai Besi, 57000 Kuala Lumpur.

Abstract. The ability to discriminate, characterise and purify biological cells from heterogeneous population of cells is fundamental to numerous prognosis and diagnosis applications; often forming the basis for current and emerging clinical protocols in stem cell therapy. Current sorting approaches exploit differences in cell density, specific immunologic targets, or receptor-ligand interactions to isolate particular cells. Identification of novel properties by which different cell types may be discerned and of new ways for their selective manipulation are clearly fundamental components for improving sorting methodologies. Biophotonics sensor developed by our team are potentially capable of discriminating cells according to their refractive index (which is highly dependable on the organelles inside the cell), size (indicator to cell stage) and shape (in certain cases as an indicator to cell type). The sensor, which already discriminate particles efficiently, is modified to acclimatize into biological environment, especially for stem cell applications.

1 Introduction

Recent derivation of human embryonic stem cell open new opportunities for regenerative medicine as well as understanding basic aspect of embryonic development and diseases such as cancers [1]. Many ideas that are now discussed have long history and much has been underpinned by the earlier studies of teratocarcinomas and embryonal carcinoma stem cells, which present a malignant surrogate for the normal stem cells of the early embryo.

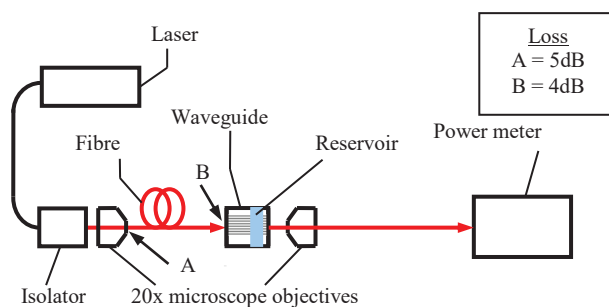


Fig. 1. Experimental set up for particle/cell trapping and propulsion

Although the potential of embryonic stem cell and embryonic carcinoma cells to differentiate into a wide range of tissue is now well attested, little is understood of the key regulatory mechanism to control their differentiation. The culture environment, morphological; all aspect plays important role in this process. Hence, there is a need for an approach to provide a pure population of stem cells that is free from mechanical

(fluid shear stress, cyclic stretch and pressure), electrical (field induced) or chemical (need for labelling) induced cellular response. Such an approach will be able to provide the effective characterization and study of different stem cell populations and ultimately clearer strategies for regenerative medicine. Optical trapping and propulsion is seen as a potential candidate as a sorting technique that avoids detrimental effects on the stem cells.

A biophotonics sensor comprises of caesium ion exchanged optical waveguides with various parameters have been developed to efficiently discriminate polystyrene particles according to their size [2]. In this paper, the system is modified to adapt into biological environment, especially for stem cell applications.

There are several characteristics needed to be investigated in order to ensure the compatibility of the system for optical trapping and propulsion of stem cells. For this purpose, characteristics of a mammalian cell type were listed. The cells should be non-adherent, at least pseudo-spherical and, if possible, have a high refractive index. Lymphoblastoma cells were seen as a good candidate not only because the cells are non-adherent and pseudo-spherical in shape, but also they are readily available and easy to culture. The investigation of optical trapping and propulsion on lymphoblastoma was carried out first, as shown in this paper, before applying the technique to teratocarcinoma cells, the cell type that is targeted for the biophotonics sensor application.

* Corresponding author: mukhzeer@upnm.edu.my

2 Experimental procedures

In order to optically propel particles and cells, a solution of particles or cells is placed in a reservoir on top of the waveguide, as illustrated in Fig. 1. The trapping and propulsion is powered by a diode pumped ytterbium doped fibre laser (IPG Photonics) operating at 1064nm. The wavelength is used as the laser source is readily available and it was proven to work for polystyrene particles propulsion on caesium ion-exchanged channel waveguides [3]. The laser source, which is linearly polarised and producing a continuous wave, is capable of supplying power up to 5W with a Gaussian output beam of 1.6mm diameter. The laser source is directed to a built-in isolator in order to provide a collimated beam and to avoid the backscatter reflection that can damage the laser source. Output from the isolator is coupled into a single mode polarisation maintaining (PM) fibre (Fibercore, HB980-T) via a 20x objective lens (loss \approx 5dB).

The PM fibre is used to adjust the input field to the optical waveguide into different polarisation modes. The PM fibre is aligned in three dimensions to give maximum output, using a fibre holder with a nanopositioner (Thorlabs - MAX313), and set to the correct polarisation using a nanorotator (Thorlabs - HFR003) attached to the fibre holder. Scattering due to Fresnel reflection is minimised by cleaving the fibre using a fibre cleaver (PK FK11). A coupling efficiency, between the fibre and the waveguide input facet, of approximately 4dB is achieved using this setup. An optical microscope was used to place the PM fibre in close proximity to the waveguide input facet. The coupling was optimised by monitoring the output of the waveguide.

Each of the experimental data was compared with a theoretical model. The theoretical model was simulated by adapting the Arbitrary Beam Theory (ABT) developed by [4, 5]. The simulation was made using the same model as in [6, 7]. Unless stated otherwise, the waveguide parameters used in the simulation were a 4 μ m channel width, a substrate index of 1.50, a waveguide index of 1.54 and a particle index of 1.59 dispersed in water (index of 1.33). The wavelength used in the simulation was 1064nm with an input power of 500mW. Note that the model assumed that there is no power loss due to the Fresnel scattering, modal mismatch or propagation loss along the channel waveguide. Furthermore, it is also assumed that the propulsion of particles is not affected by any non-optical forces.

3 Results and discussion

3.1 Particle/cell size matching

With a view to apply the existing system in the trapping and propulsion of particles to mammalian cells, certain characteristics of the mammalian cells can be investigated using particles of a similar property. One of the characteristics that can be investigated using particles

is the cell size. The diameter of the cell used varies depending on its type and the state of the cell cycle. Lymphoblastoma cells can vary from approximately 8 μ m to 12 μ m, while teratocarcinoma cells vary from 15 μ m to 23 μ m. In order to evaluate the effect of varying cell size, six different polystyrene particle sizes, ranging from 1 μ m to 20 μ m diameter, were used. The propulsion velocity of each particle size was measured using a 12 hour caesium ion-exchanged waveguide [2].

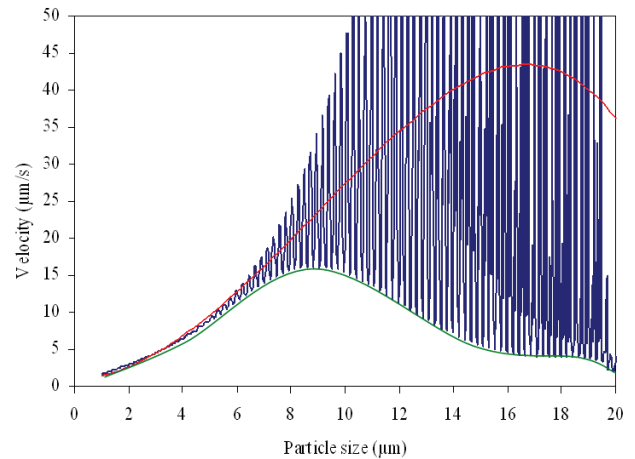


Fig. 2. Theoretical model of the propulsion velocity of varying particle sizes at TM mode. The red line indicates the best fit between the two adjacent maxima and minima in the theoretical model and the green line is the estimated non-resonance propulsion estimation

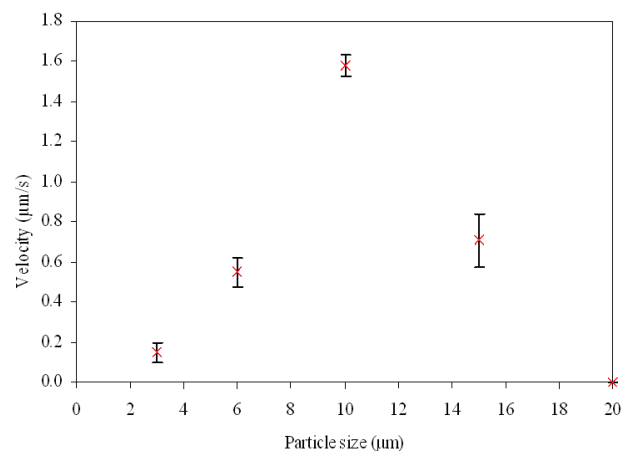


Fig. 3. Propulsion velocity of varying polystyrene particle sizes

Fig. 2 illustrates the theoretical model of the propulsion velocity for varying particle sizes. The theoretical plot shows velocity resonance, an effect that is observed in total scattering and extinction cross-sections for Mie particles [8, 9]. These resonances originate from the electromagnetic modes of a sphere and are known as Morphology Dependent Resonances (MDRs) [8, 9]. With increasing radius, the loss for the internal field decreases, the internal field accumulates and resonances occur [7]. Note that the resonances become narrower with particle size. This indicates that the condition for resonance is harder to satisfy for larger particle size. There are a few limitations for the theoretical model to be met experimentally. The model assumes a lossless particle where the particle is assumed

to be a perfect sphere and of high quality factor, Q . These particle characteristics are not met with the particles used in this experiment. Furthermore, the laser is assumed to be an ideal laser of a single frequency linewidth.

The experimental data is illustrated in Fig. 3. The propulsion velocity was observed to increase with particle size. However, the $15\mu\text{m}$ particles show reduction in velocity and no propulsion observed for $20\mu\text{m}$ particles. An increase in the particle size increases the polarizability of the particle and the optical force. The scattering image from a $20\mu\text{m}$ particle proves that there was optical force acting on the particle although no propulsion was observed. There was also no apparent propulsion for $1\mu\text{m}$ particles observed in the experiments, mostly due to the limitation of the lenses available to monitor and track the $1\mu\text{m}$ particles. However, lateral trapping of the particles can be detected. The increment in the intensity line profile indicates an increasing number of $1\mu\text{m}$ particles trapped in the illuminated channel with increasing time. As indicated in previous papers [10-12], the Brownian motion is more apparent as the size of the particles decreases. The $1\mu\text{m}$ particles were seen to move randomly in Brownian motion. However the motion was directed to the illuminated channel, indicating a strong lateral trapping.

There are some discrepancies between experimental velocities and the predicted velocity in the theory. Apart from the reasons stated previously, the standard deviation of the particles used was observed to be higher than the distance between two adjacent maxima and minima of the velocity resonance. For example, the standard deviation for a $10\mu\text{m}$ particle is $0.763\mu\text{m}$ while the difference between maximum and minimum near $10\mu\text{m}$ particle size is $0.06\mu\text{m}$ in the theoretical plot. In addition, small deviations from spherical symmetry are known to affect the quality factor of the narrowest resonances [13]. Therefore this may indicate that the particles that were used in the experiments are not perfectly spherical. Hence, the experiments did not observed a wide range of propulsion velocities as expected from the theory. In addition, estimation of mammalian cell propulsion using the theoretical model is also invalid. Mammalian cells were observed to be hemispherical on surface [2], which indirectly increases the frictional force due to a larger contact area. However, assuming non-resonance propulsion estimation, as illustrated in Fig. 2, the trend of particles propulsion observed in the experiments follows the theory. This might be a better approximation to estimate the propulsion velocity according to size. The theory should also taken into consideration the reduction of laser power due to modal mismatch, scattering and Fresnel reflection.

3.2 Refractive index variation

Apart from differences in size, density, structure and surface properties, cells also have a low refractive index compared to the polystyrene particles. A variation in the

refractive index changes the propulsion behavior of the cells. The refractive index of the polystyrene particles used in all experiments is $n=1.59$. Exact values of the refractive index of lymphoblastoma cells or teratocarcinoma cells on the other hand could not be found in the literature. However, as most of the cell structure consists of cytoplasm, it is fair to assume that the refractive index will be close to $n\approx 1.39$, as indicated in [14, 15]. Prior to manipulation of cells, propulsion of particles with the refractive index close to the cell index was investigated to predict the propulsion behavior of a low index material.

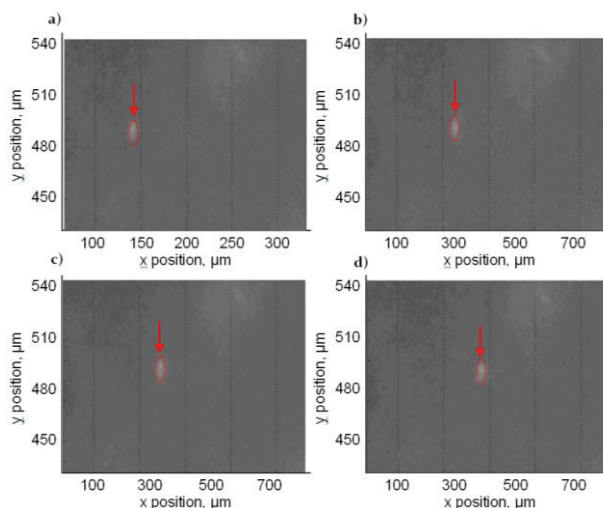


Fig. 4. Propulsion of PMMA particles a) Image taken at $t = 0\text{s}$, b) $t = 66\text{s}$, c) $t = 133\text{s}$ and d) $t = 200\text{s}$

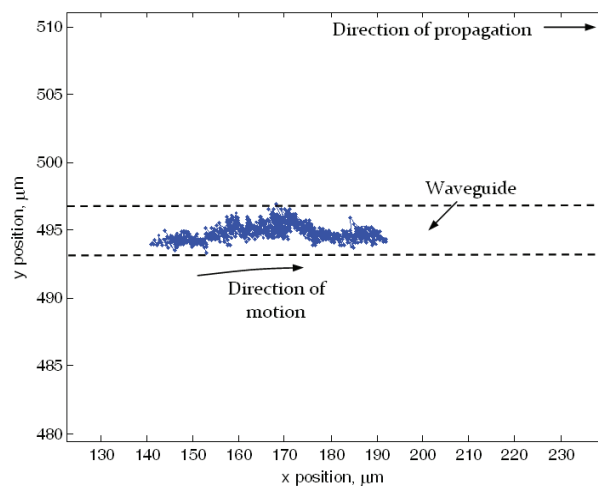


Fig. 5. Output from the particle tracking software. PMMA particle propulsion is presented in ■ coloured line

The lowest refractive index available commercially is obtained from silica spheres, which is approximately 1.46. The refractive index is the closest to the assumed refractive index of mammalian cells; unfortunately the particle is quite dense with the density of 2.5gcm^{-3} . A high density particle has a larger mass (hence, more friction force) and preliminary propulsion experiments using silica spheres show no motion at all [2]. Hence, $10\mu\text{m}$ diameter polymethylmethacrylate (PMMA)

particles with a refractive index of 1.489 were chosen [16]. The same optical and waveguide setup was used to carry out trapping and propulsion analysis of PMMA particles. A series of images of PMMA particles propulsion is shown in Fig. 4. The images were compressed (in the x -direction) in order to accommodate the distance travelled by the particle. The sequence of images in Fig. 4 shows that the PMMA particle moved with a mean velocity of $0.23 \pm 0.07 \mu\text{m/s}$. As illustrated in Fig. 5, Brownian motion was more pronounced in the PMMA particle propulsion vis-à-vis the observation for the polystyrene particles. This is due to the lower refractive index of the PMMA particles. This investigation was extended by varying the input power supplied to the $4 \mu\text{m}$ nominal width channel waveguide.

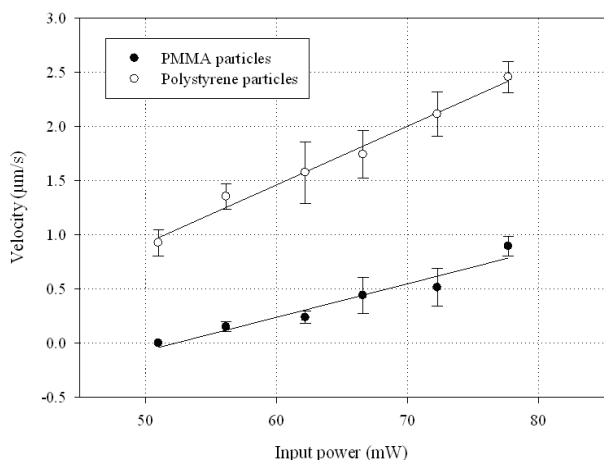


Fig. 6. Propulsion velocity of $10 \mu\text{m}$ PMMA particles with varying input power. Propulsion velocity of polystyrene particles of the same size is also plotted for comparison

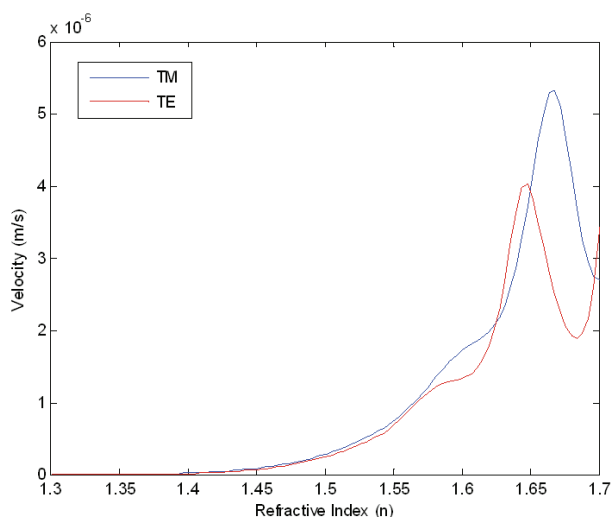


Fig. 7. Theoretical velocity of particles with varying refractive index

Fig. 6 shows the velocity of $10 \mu\text{m}$ PMMA particles on the 12 hour caesium ion-exchanged waveguide. The input power was varied from about 400mW up to 620mW by adjusting the current supplied to the laser (corresponds to 50mW to 78mW input power to the waveguide). Propulsion of a $10 \mu\text{m}$ polystyrene particle

on the same waveguide is also plotted on the same graph for comparison. The propulsion for PMMA particles is clearly much less than for the polystyrene particle in all ranges of input power tested, as expected from the theoretical model in Fig. 7. PMMA particles were also observed to be unable of propulsion at about 50mW input power. This may indicate the minimum threshold power needed for PMMA particle's propulsion. At similar input powers, polystyrene particles propel, on average, at a velocity of $0.93 \mu\text{m/s}$. PMMA and polystyrene particles propel with a mean velocity of $0.24 \mu\text{m/s}$ and $1.58 \mu\text{m/s}$ respectively with an input power of approximately 66mW .

In order to understand the effect of different refractive indices of particles, a simulation using the same model as in [6, 7] was carried out. The same optical and waveguide arrangement, as described earlier in this section, was set in the simulation. The simulated velocity for polystyrene particles was normalized to the experimental values in order to have a more realistic estimation of the propulsion velocity of PMMA particles. The predicted particle velocity against the particle's refractive index is illustrated in Fig. 7. The simulation indicates that higher propulsion velocity is achieved at the TM mode compared to the TE mode for the particles under consideration (refractive index less than $n=1.6$) as predicted in previous papers [10-12]. The velocity for the PMMA particle is expected to be around $0.2266 \mu\text{m/s}$ due to a lower effective index which approximately the same as observed experimentally. The observations on varying particle size and refractive index suggest that the propulsion of mammalian cells of interest, lymphoblastoma and teratocarcinoma cells was indeed feasible. The size range of the mammalian cells overlaps the size range of particles that could be propelled on the caesium ion-exchanged waveguide. The theoretical model, as illustrated in Fig. 7, also shows the predicted velocity for cells of refractive index near 1.39, which is about 6.273nm/s .

3.3 Effect of surface functionalization

Mammalian cells involved in this project are lymphoblastoma and two types of teratocarcinoma cells; TERA1 and NT2 cells. Although lymphoblastoma grows in suspension and is less likely to adhere to the surface, teratocarcinoma cells adhere to the surface and form a monolayer in culture. Thus, a method to reduce adhesion and promote the dominance of a double layer repulsive force is by functionalizing the waveguide surface. A 12 hour caesium ion-exchanged waveguide was PEG-functionalized, as detailed in [2]. Prior to the functionalization step, propulsion experiments of $8 \mu\text{m}$, $10 \mu\text{m}$ and $12 \mu\text{m}$ polystyrene particles were carried out on the waveguide for comparison. Fig. 8 shows results from the propulsion experiments on both PEG-functionalized and plain surfaces.

It can be observed in the propulsion experiments that particles of all sizes tested show a faster propulsion

on the PEG-functionalised surface. From Fig. 8, propulsion of polystyrene particles is on average 25% faster than propulsion on a plain surface. Apart from preventing cell adhesion [17, 18], the faster propulsion observed also indicates a reduction in the frictional force that is opposing the particle motion, as discussed in [12]. This is beneficial in terms of applying the system to propel mammalian cells since a low refractive index is expected to reduce the propulsion velocity dramatically. Any minimization of forces that hinder the propulsion (frictional force and cell adhesion) is definitely seen as an advantage.

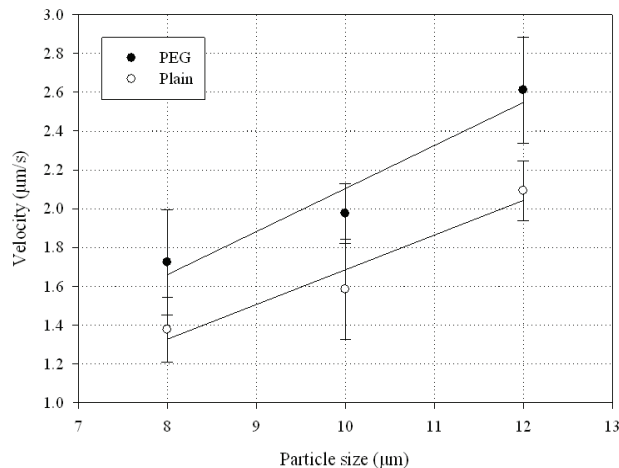


Fig. 8. Propulsion of 8µm, 10µm and 12µm polystyrene particles on PEG-functionalized and plain waveguide surfaces

4 Conclusion

The optical trapping and propulsion of polymer particles, namely polystyrene and PMMA were presented in this paper. Biological cells not only vary in terms of size and refractive index but also their surface characteristics. Hence, the propulsion of polymer particles of varying sizes and refractive indexes were investigated initially on plain and functionalized surfaces of caesium ion-exchanged waveguides. It was found that as the refractive index of the particles decreased, the propulsion velocity was also observed to decrease, as demonstrated by the PMMA particles (propulsion rate of $3.9 \times 10^{-3} \mu\text{ms}^{-1} \text{mW}^{-1}$). The investigation of different surfaces showed that the propulsion velocity of particles on a PEG-functionalized surface increased on average by 25%.

The work carried out here determined the optimum optical, waveguide parameters and surface characteristics to be further exploited for trapping and sorting of teratocarcinoma cells and ultimately stem cells on caesium ion-exchanged channel waveguides. These studies on biophotonics sensor is expected to provide a fast, reliable and high throughput discriminating mechanism that is practical and applicable to real environment in the future.

References

1. J. A. Thomson, *Science*, **282**, pp. 1827-1827 (1998)
2. M. M. Shahimin, "Propulsion of polymer particles on caesium ion-exchanged channel waveguides for stem cell sorting applications," in *School of Electronics and Computer Sciences*. PhD Thesis Southampton: University of Southampton, pp. 1-206 (2009)
3. K. Grujic, O. G. Hellese, J. S. Wilkinson, and J. P. Hole, *Optics Communications*, **239**, pp. 227-235 (2004)
4. J. P. Barton, D. R. Alexander, and S. A. Schaub, *Journal of Applied Physics*, **64**, p. 1632 (1988)
5. J. P. Barton, D. R. Alexander, and S. A. Schaub, *Journal of Applied Physics*, **66**, p. 4594 (1989)
6. H. Jaising, K. Grujic, and O. G. Hellese, *Optical Review*, **12**, p. 4 (2005)
7. H. Y. Jaising and O. G. Hellese, *Optics Communications*, **246**, pp. 373-83 (2005)
8. C. F. Bohren and D. R. Huffman, *Absorption and scattering of light by small particles*, (John Wiley & Sons, New York, 1983)
9. Y. Panitchob, G. Senthil Murugan, M. N. Zervas, P. Horak, S. Berneschi, S. Pelli, G. Nunzi Conti, and J. S. Wilkinson, *Optics Express*, **16**, pp. 11066-11076 (2008)
10. M. M. Shahimin, O. G. Hellese, J. S. Wilkinson, and T. Melvin, *Proceedings of 25th Regional Conference on Solid State Science and Technology* (2009)
11. M. M. Shahimin, O. G. Hellese, J. S. Wilkinson, and T. Melvin, *Proceedings of Nanomaterials Synthesis and Characterisation Conference* (2009)
12. M. M. Shahimin, O. G. Hellese, J. S. Wilkinson, and T. Melvin, *Proceedings of Malaysian Technical Universities Conference on Engineering and Technology* (2009)
13. M. I. Mishchenko and A. A. Lacin, *Applied Optics*, **42**, pp. 5551-5556 (2003)
14. S. R. Goodman, *Medical cell biology*. (Alabama: J B Lippincott Company, 1994)
15. E. D. P. DeRobertis, F. A. Saez, and E. M. F. J. DeRobertis, *Cell biology* (6th ed. Philadelphia: W B Saunders Company, 1975)
16. Microparticles GmbH Berlin, *Poly(methyl methacrylate) Particles: Physical and Chemical Properties* (2008)
17. S. Mandal, J. M. Rouillard, O. Srivannavit, and E. Gulari, *Biotechnology Progress*, **23**, p. 972 (2007)
18. A. Wolter, R. Niessner, and M. Seidel, *Analytical Chemistry*, **79**, p. 4529 (2007)
19. J. P. Hole, J. S. Wilkinson, K. Grujic, and O. G. Hellese, *Conference on Lasers and Electro-Optics (CLEO 2005)* (2005)